UNIVERSITY OF CRETE

DEPARTMENT OF BIOLOGY

SCHOOL OF MEDICINE

FOUNDATION FOR RESEARCH AND TECHNOLOGY

INSTITUTE OF MOLECULAR BIOLOGY AND BIOTECHNOLOGY

M.Sc. MOLECULAR BIOLOGY & BIOMEDICINE

"Promyelocytic Leukemia Protein (PML) Regulates Epithelial – Mesenchymal Transition & Tumorigenicity in Breast Cancer Models"

Myrsini Anastasia Dimakopoulou

Supervisors:

Princ. Researcher Androniki Kretsovali

Assistant Prof. C. Nikolaou

Emeritus Prof. J. Papamatheakis

Heraklion

October, 2019

Acknowledgments

The present study was accomplished at the Institute of Molecular Biology and Biotechnology in the Foundation for Research and Technology, Heraklion, Crete in collaboration with the Computational Genomics Group in Biology Department, University of Crete. As the two years of my master studies come to an end, I would like to thank all the people that stood by me along this journey.

First of all, I would like to thank my supervisor Prof. Joseph Papamatheakis, my co-supervisor Assistant Prof. Christoforos Nikolaou, as well as Dr. Androniki Kretsovali for giving me the opportunity to work in their labs. Their guidance and their scientific advices helped me go deeper in the understanding of biology and taught me the most important feature of a biologist, the scientific way of thinking.

Furthermore, a great thank to all the people I collaborated with in both labs:

A very special thank to Mr. Takis Makatounakis, our lab technician, the “heart” of the lab and one of the most kind and patient man I’ve met. I am grateful for all the experimental techniques and the clever tricks he taught me throughout this year. I am also thankful to Amalia Vogiatzoglou for her constant help and guidance. It wouldn’t be the same without our conversations, trying to figure out what the next step of our study should be. Although we didn’t work together, I also owe a thank to Nikoleta for introducing me to the subject, as well as to our undergraduate student Konstantinos and all the master students that worked with us for short periods. It was a great lack for me to work in such a supportive environment, with pleasant collaborators.

I would also like to express my special gratitude to all the members of the CG^2 group. Lydia, Stelios, Emilios and Konstantinos, as well as all the rotators contributed to form the most warm and friendly working environment. A special thank to Antonis Klonizakis not only for being a good friend, but also for the willingness to help me anytime I needed and to answer all my questions.

A wholehearted thank to my very best friends and fellow students: Mantha, Irene, Ioanna, Antonis and Dimitris. We started together our master studies, we encouraged and supported each other and we shared beautiful moments, but also some of the hardest that bonded our friendship. The last two years wouldn’t be the same without them.

Finally, I would like to thank my parents, Eleni and Giorgos, and my sisters, Despina and Ariadni, for their constant support and encouragement throughout my six years of undergraduate and master studies here, in the beautiful island of Crete.

Contents

Abstract

Promyelocytic leukemia protein (PML) is a multifunctional protein, as it is implicated in a wide range of biological processes, including DNA – damage response, apoptosis, senescence and angiogenesis. PML also displays a contradictory role in the development of cancer, as both tumor – suppressor and pro - survival roles have been attributed to its function, depending the system of study. Here, we compare two breast cancer cell lines: the triple-negative, mesenchymal MDA.MB.231 and the luminal A, epithelial MCF7 in order to detect the effect of PML silencing in cell growth, epithelial-mesenchymal transition and tumorigenisity. Through *in vitro* cultures and an *in vivo* mouse experimental model it is shown that upon PML knockdown MDA.MB.231 favor a more aggressive character, with a higher capability to form tumors and metastatic foci, whereas MCF7 tend to acquire a mesenchymal phenotype with increased migratory and invasive ability.

Περίληψη

Η πρωτεΐνη προμυελοκυτταρικής λευχαιμίας (PML) συμμετέχει σε μια πληθώρα βιολογικών διεργασιών, συμπεριλαμβανομένων της επιδιόρθωσης DNA βλαβών, της απόπτωσης, της κυτταρικής γήρανσης και της αγγειογένεσης. Συμμετέχει επίσης, στην εξέλιξη του καρκίνου παρουσιάζοντας ωστόσο αντιφατική δράση: αναλόγως το υπό μελέτη σύστημα έχει βρεθεί να δρα είτε ογκο-κατασταλτικά, είτε ως ορογόνος πρωτεΐνη. Στην συγκεκριμένη εργασία συγκρίθηκαν δύο κυτταρικοί τύποι καρκίνου του μαστού: τα τριπλά – αρνητικά και μεσεγχυματικού χαρακτήρα MDA.MB.231, καθώς και τα luminal A, επιθηλιακού τύπου MCF7. Μέσω *in vitro* κυτταρικών καλλιεργειών και *in vivo* πειραμάτων σε ποντίκια, μελετήθηκε η επίδραση της αποσιώπησης της PML και διαπιστώθηκε ότι τα MDA.MB.231 κύτταρα τείνουν να εμφανίζουν έναν πιο επιθετικό χαρακτήρα, ενισχύοντας την ικανότητά τους προς σχηματισμό όγκων και μεταστασεων, ενώ τα MCF7 κύτταρα φαίνεται να αποκτούν έναν πιο μεσεγχυματικό φαινότυπο, με αυξημένη δυνατότητα για μετάσταση και διήθηση.

1. Introduction

1.1 Promyelocytic Leukemia Protein

PML was first identified in Acute Promyelocytic Leukemia (APL) patients, as a chimeric transcript encoded from a genetic locus at the breakpoint of t(15;17) chromosomal translocation along with the Retinoic Acid Receptor a (RARa) gene (A. Kakizuka 1991, The 1991).The fused PML – RARa protein displays oncogenic properties and disrupts the physiological functions of both proteins, that is the organization of subnuclear domains linked to post – translational modifications and the regulation of myeloid differentiation, respectively. In APL cells the expression of PML – RARa chimera prevents myeloid differentiation, whereas myeloid progenitors exhibit enhanced self – renewal capacity and resistance to apoptosis (de The and Chen 2010).

The PML gene is located on chromosome 15 in humans and gives rise to a variety of alternatively spliced mRNA transcripts and multiple protein isoforms. The first three exons of its N – terminal region encode for three cysteine – rich zinc – binding domains, a RING finger, two B – boxes (B1 and B2) and an a–helical Coiled – Coil domain, which together form the common for all PML isoforms RBCC/TRIM motif (Fagioli et al. 1992). Besides this motif, almost all PML isoforms contain a nuclear localization signal (NLS) and three lysine residues (position 65 in the RING finger, 160 in the B1 box and 490 in the NLS) available for SUMO modification (Tetsu Kamitani and Yeh 1998). The PML isoforms differ in the central region or in the C – terminal region and according to these sequence differences are categorized in seven groups (PML I – VII), which can be further sub-categorized to a/b/c variants (Figure 1.1) (de The et al. 1991, Fagioli et al. 1992). The size of the isoforms varies from 435 to 882 amino acids and the variation of C – termini enhances interactions with different molecules, thus providing the diverse function of each isoform. Almost all isoforms reside in the nucleus, whereas PML VII, lacking the NLS sequence remains cytoplasmic. Furthermore, PML I is capable of nucleus to cytoplasm and vice versa translocation, as it contains a nuclear export signal (NES) in exon 9 (Kirsten Jensen 2001).

1.2 PML Regulation

In order to sustain a steady – state expression of PML in every tissue, PML is regulated in transcriptional, post – transcriptional and post – translational level.

Transcriptional regulation of PML concerns cytokine mediated signaling, such as IFNS, TNFa and IL-6. Specifically, type I and type II interferons (IFNs) are able to regulate PML transcription by activating the Janus kinase/signal transducer and activator of transcription (JAK/STAT) pathway (Chelbi-Alix et al. 1995, Pelicano et al. 1995). Stats and interferon – induced regulatory factors (IRF8 and IRF3) bind IFN – responsive cis elements in the PML promoter, including ISRE and GAS, and activate PML transcription

(Hsu and Kao 2018). Interleukin 6 (IL-6) also enhances PML expression through JAK/STAT, as well as the NF-κB pathway (Hubackova, Krejcikova et al. 2012), while tumor necrosis factor a (TNFa) up – regulates PML mRNA levels through STAT1 in endothelial cells (Cheng, Liu et al. 2012). Furthermore, p53 induces PML expression via consensus p53 response elements in the PML first intron, in response to oncogenes and DNA damage (Elisa de Stanchina, Pier Paolo Pandolfi et al. 2004). On the other hand, Stat3 and Stat6 have been found to suppress PML expression during mammary gland development (Hsu and Kao 2018).

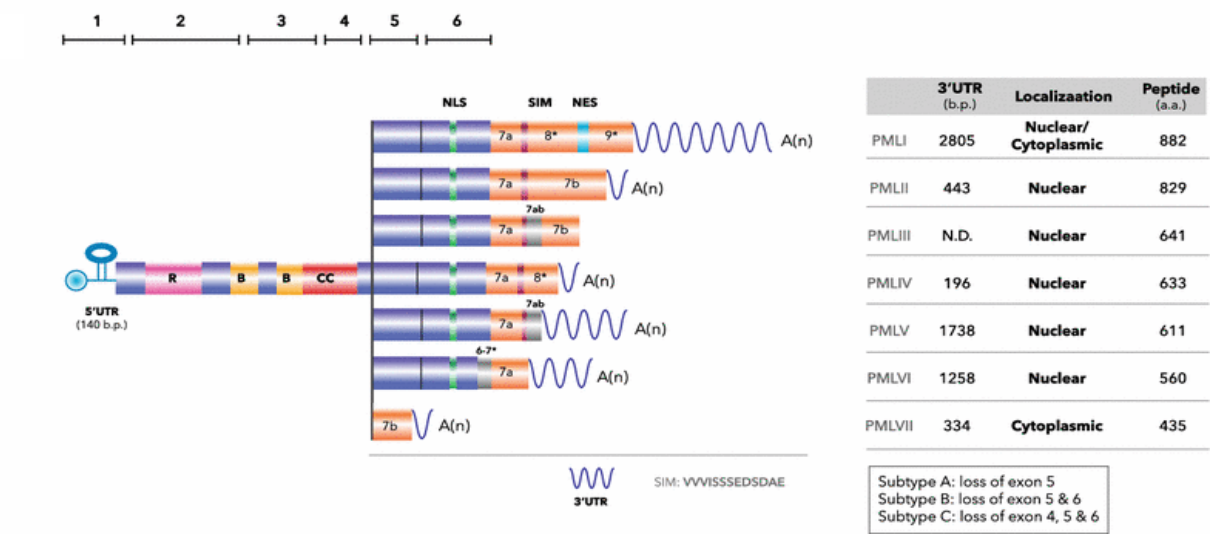

	3'UTR (b.p.)	Localizaation	Peptide (a.a.)
PMLI	2805	Nuclear/ Cytoplasmic	882
PMLII	443	Nuclear	829
PMLIII	N.D.	Nuclear	641
PMLIV	196	Nuclear	633
PMLV	1738	Nuclear	611
PMLVI	1258	Nuclear	560
PMLVII	334	Cytoplasmic	435

Subtype A: loss of exon 5
Subtype B: loss of exon 5 & 6
Subtype C: loss of exon 4, 5 & 6

Figure 1.1: **Structure of the PML isoforms**: Seven main PML isoforms arise by alternative splicing of nine exons. Each isoform can be further classified to a, b or c subtypes. While all of them contain a stable N – terminal region, they are distinguished according to their variable C – termini, which also mediate their wide spectrum of protein - protein interactions (Hsu and Kao 2018).

PML is post – transcriptionally regulated through alternative splicing, giving rise to the six nuclear and one cytoplasmic isoform. Each one of them displays distinct functions, as for example PML III controls centrosome duplication, PML IV, which is the most studied, interacts with a variety of proteins including p53, TERT (telomerase reverse transcriptase), TIP60 (histone acetyl transferase) and stabilizes c-Myc and the cytoplasmic PML VII implicates in cytokine signaling, apoptosis and antiviral defense (Nisole, Maroui et al. 2013).

Furthermore, PML isoforms undergo post – translational modifications, which can regulate their stability, localization and function. First of all, PML is SUMOylated through the addition of small ubiquitin – like modifier proteins (SUMO) in several lysine residues, including the three major SUMOylation sites K65, K160 and K490. SUMO modification is mediated by non-covalent SUMO biding or covalently through the E1, E2, E3 enzymatic cascade. Depending on the stimuli SUMOylation can

either be a negative or a positive regulator of PML levels, as it can activate the ubiquitin – dependent degradation or prevent the phosphorylation – mediated degradation, respectively. Phosphorylation of PML, in response to growth factors or stress conditions, can lead to opposite effects, promoting protein degradation or in some cases stabilization. The degradation of PML is accomplished by ubiquitination with at least seven E3 ligases and activation of the proteasome pathway (Hsu and Kao 2018).

1.3 PML NBs

PML is essential for the formation of subnuclear domains called PML Nuclear Bodies (PML - NBs). They are spherical, discrete nuclear foci, varying in size from 0.2 to 1.0μm, ranging from 1 to 30 bodies per nucleus, depending on the cell type, cell cycle phase and differentiation stage. PML – NBs are present in most mammalian cells, however display functional and structural heterogeneity and characterized as dynamic structures. Besides NBs, PML proteins are also found in the nucleoplasm, implying a dynamic exchange between NB - bound and diffused form. Structurally, PML-NBs are composed by a PML – formed ring at the periphery, whereas the inner core of the structure contains a wide range of proteins that have been found to directly or indirectly interact with PML. More than 170 proteins reside either constantly or transiently in PML-NBs, including transcription factors, cofactors, DNA repair proteins and post – translational modifiers.

Due to the extended list of PML-NBs partners, they are found to participate in several biochemical activities, such as DNA repair, replication and transcription, mRNA export, apoptosis, cellular senescence, cell proliferation and maintenance of genomic stability. Moreover, PML-NBs undergo through several changes during cell – cycle progression. G0 cells contain few NBs, while their number rises in G1 and even more in S and G2 phases. During S phase the retraction of chromatin from NBs in order to replicate leads to fragmentation of NBs, which in turn accumulate into larger and fewer aggregates during chromatin condensation in mitosis. Mitotic accumulation of PML proteins (MAPPs) differ in terms of biochemical composition from interphase PML - NBs and they are implicated in the reformation of the nuclear envelope (Bernardi and Pandolfi 2007, Borden 2008).

PML –NB assembly involves, firstly, the formation of the outer NB shell by covalent multimerization of oxidized PML monomers, as well as non-covalent homodimerization through the RBCC/TRIM motif. Subsequently, SIM – containing partners bound the different PML isoforms in the periphery through SUMO/SIM interactions giving rise to the mature PML-NB (Figure 1.2). Thus, PML- NBs serve as hubs and catalytic platforms for the accumulation of various regulatory proteins, contributing to their functionality in several processes (Bernardi and Pandolfi 2007, Hoischen, Monajembashi et al. 2018).

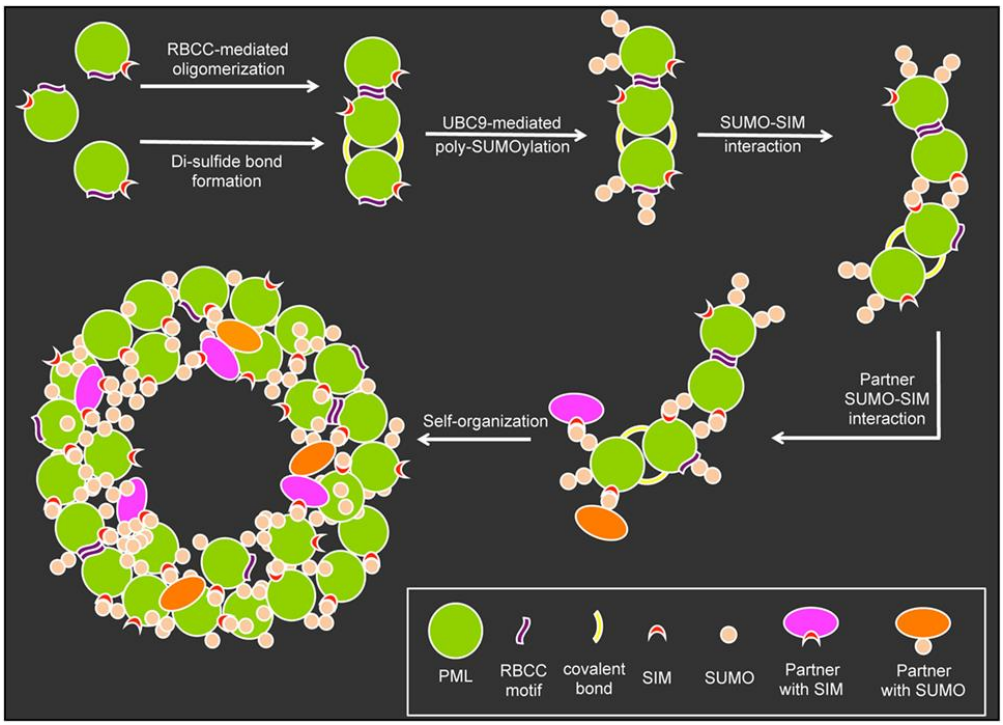

Figure 1.2: **Assembly of PML Nuclear Bodies**: The formation of PML-NBs requires covalent and non-covalent interactions of PML molecules. Initially, non-SUMOylated PML monomers oligomerize through weak interactions, formed by the RBCC motif. Subsequently, SUMOylation enables the assembly of larger entities by SUMO – SIM interactions and, finally, the recruitment of binding partners reinforces the formation of the mature PML body (Hoischen, Monajembashi et al. 2018).

1.4 Multifunctional role of PML

As mentioned above, PML and PML-NBs have been linked to many biological aspects, all of them leading eventually to the maintenance of genome stability. In particular, PML-NBs are implicated in DNA damage responses, as many DNA repair and checkpoint proteins have been found to interact with them and their number tends to increase in an ATM or ATR-dependent way. Their exact role in DNA repair has not been clarified, but the idea is that PML-NBs serve as storage sites that release checkpoint proteins after DNA damage and they mediate the association of DNA repair with checkpoint response (Bernardi and Pandolfi 2007, Hoischen, Monajembashi et al. 2018).

Additionally, PML is connected to both p53 - dependent and p53 - independent pathways of apoptosis. p53 is recruited in PML-NBs, where its expression is activated by post-translational modifications. On the other hand, PML interacts with other apoptosis – promoting proteins, such as Fas and DAXX, in the NBs driving to apoptotic functions. As far as about senescence, PML-NBs have been found to implicate in

chromatin modifications in order to form senescence associated heterochromatin foci (SAHF), that silence growth related genes (Bernardi and Pandolfi 2007).

PML has also been associated with transcriptional regulation however it is unclear whether the diffused or the NB-bound form of PML provides this feature. PML bounds to various gene promoters and functions as a co-activator or a co-suppressor of mRNA expression. Apart from that, PML can interact and activate other transcriptional cofactors. The opposite activities of PML can be explained either due to the heterogeneity of PML-NB interacting partners, or because PML-NBs alter their localization in the nucleus during cell cycle or upon extracellular stimuli (Bernardi and Pandolfi 2007).

1.5 PML in tumorigenesis

The involvement of PML in several, often contradictory, biological pathways has led to the notion that it may have a dual role in tumorigenesis. PML was firstly characterized as a tumor – suppressor gene, due to several data showing its implication in anti – oncogenic processes. In particular, PML promotes senescence along the pRb and p53 tumor suppressive pathways. It also induces apoptosis through acetylation and activation of p53, as well as through p53 – independent manner. The tumor – suppressing function is possibly related to the accumulation and stabilization of DNA damage response proteins in PML-NBs (Martin-Martin, Sutherland et al. 2013, Mazza and Pelicci 2013, Sahin, Lallemand-Breitenbach et al. 2014, Hoischen, Monajembashi et al. 2018).

In spite of its tumor – suppressive functions, PML has been shown to preserve oncogenic potentials. The pro-survival role was initially described in cells from chronic myeloid leukemia (CML) patients and further observed in hematopoietic stem cells (HSCs) through regulation of fatty acid oxidation (FAO) by PML. FAO regulates the balance between quiescence and cell cycle progression under the control of peroxisome-proliferator activated receptor δ (PPARδ). PML is required for HSCs for control of HSC asymmetric division, acting upstream of this pathway (Martin-Martin, Sutherland et al. 2013, Hoischen, Monajembashi et al. 2018). Moreover, studying PML in breast cancer biopsies showed elevated levels of PML mRNA and protein levels in TNBC cells. This is relevant to the pro-survival role of PML through the PPARδ - FAO pathway, under stress conditions due to loss of attachment in breast cancer cells (Carracedo, Weiss et al. 2012, Mazza and Pelicci 2013).

In this concept, it has been suggested that PML acts both as a tumor – suppressor and an oncogene, depending on the cell context. It can promote self-renewal of CML cells and avoid anoikis in TNBCs regarding to the pro-survival function, whereas it promotes cell cycle arrest, apoptosis, senescence and prevents angiogenesis when acting as a tumor-suppressor (Figure 1.3).

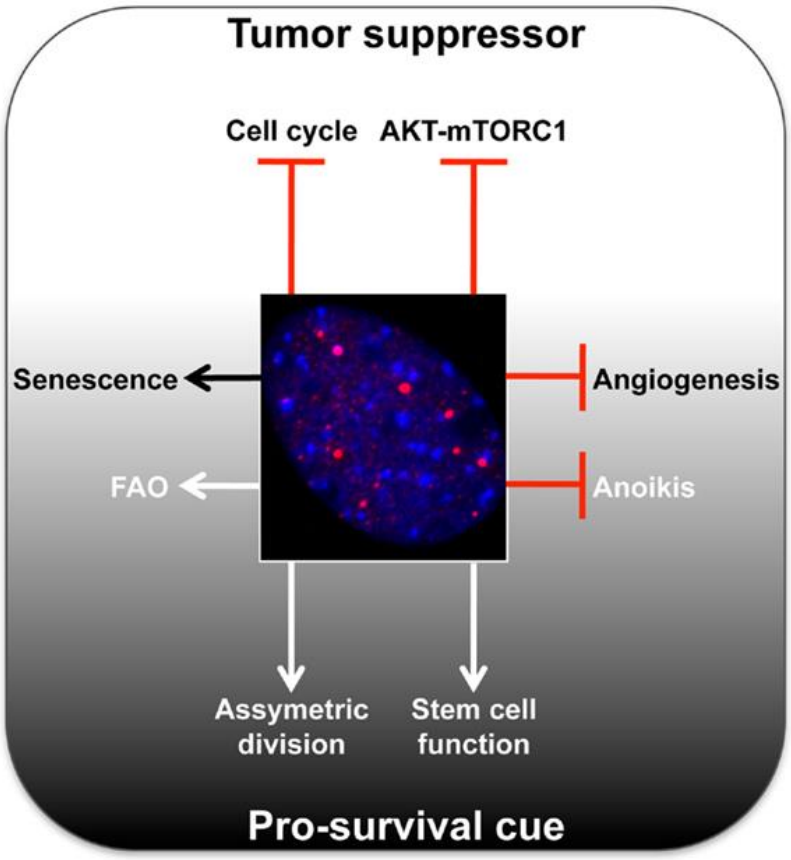

Figure 1.3: **Dual role of PML in cancer progression:** PML is able to act either as a pro – apoptotic or as a pro – survival factor, through regulation of variable biological processes (Martin-Martin, Sutherland et al. 2013).

1.6 Breast cancer

Breast cancers are categorized into five groups, in order to stratify patients for predictions and treatments, known as "intrinsic subtypes of breast cancer". According to gene expression clustering they are classified into five molecular subtypes: Luminal A, Luminal B, HER2 enriched, Claudin – low and Basal – like, as well as a Normal Breast-like group, with diverse responses to treatments and survival potential.

Claudin-low tumors, also known as Triple Negative Breast Cancer (TNBC), lack the expression of estrogen receptor (ER-), progesterone receptor (PR-) and human epidermal growth factor receptor 2 (HER2-). Both claudin-low and basal-like subtypes are characterized by low expression of HER2 and luminal gene clusters. However, claudin-low subtype expresses reduced levels of cell – cell adhesion proteins, including claudins that participate in the formation of tight junctions and E-cadherins, as well as low levels of proliferation related genes. In the same time, claudin - low group has been found to highly express genes related to immune responses and mesenchymal or extracellular genes. Due to this

specific expression pattern claudin-low tumors display high mesenchymal features and low luminal/epithelial differentiation (Prat and Perou 2011).

As far as luminal A and B subtypes (hormone receptor-positive and HER2-negative), they are distinguished based on the expression levels of particular gene groups. Specifically, luminal A subtype expresses higher levels of luminal and hormone regulated genes, lower levels of proliferation and cell – cycle related genes and contain fewer mutations throughout their genome in comparison to luminal B subtype. Accordingly, HER2 – enriched subtype expresses high levels of HER2 and proliferation genes, as well as intermediate levels of luminal genes. Finally, the basal – like subtype is characterized by high expression levels of proliferation related genes, intermediate levels of HER2 related genes and low levels of luminal related genes (Prat, Pineda et al. 2015).

1.7 Epithelial – Mesenchymal Transition

The phenomenon of epithelial – mesenchymal transition (EMT) had been firstly characterized in early 1980s during development of chick embryos (Hay 1995). Further studies revealed the loss of epithelial traits and the concomitant acquisition of mesenchymal traits is a common mechanism of epithelial cells, observed in various processes including tissue repair, inflammation, fibrosis and cancer progression. Also, the ability of mesenchymal cells to turn to epithelial, termed mesenchymal – epithelial transition (MET), illustrates the plasticity of epithelial phenotype (Chen, You et al. 2017).

Epithelial cells are closely linked to their neighbors, forming apical – basal polarized sheets. Cells are connected through cell-adhesion molecules such as E-cadherin and claudin, giving rise to junctions associated with cytoskeleton, including tight, adherens and gap junctions, as well as desmosomes. Through the basal membrane they form interactions with the extracellular matrix, mediated by substrate-adhesion molecules, such as the a6β1 and a6β4 integrins. Mesenchymal cells, on the other hand, present end – back polarity and form transient contacts with their neighbors (Gonzalez and Medici 2014).

The main hallmark of EMT is the reduction in the expression of epithelial markers, such as E-cadherin, occludin and cytokeratins, while mesenchymal markers such as vimentin, fibronectin and N-cadherin are induced. These expression changes are guided by several transcription factors, including the zinc-finger binding factors Snail1 and Snail2, the zinc-finger E-box-binding proteins Zeb1 and Zeb2, as well as the basic helix-loop-helix (bHLH) factors Twist. All these master EMT transcription factors contribute at different extend, depending the cell or tissue type, by binding the promoter regions and repress the expression of epithelial genes (Gonzalez and Medici 2014, Diepenbruck and Christofori 2016).

Besides the implication in physiological processes, EMT is also related with cancer metastasis. According to the “plasticity type I” metastasis model, tumor cells undergo EMT and form low proliferative mesenchymal cells with increased migratory and invasive properties. Eventually, mesenchymal cells undergo MET and form metastases in distant organs, characterized by the presence of both epithelial

and mesenchymal cells. The “genetic type II” model, on the other hand, supports that tumor cells undergo a permanent transition, accompanied by loss of cell plasticity and acquisition of stem-like properties (Figure 1.4) (Bill and Christofori 2015, Diepenbruck and Christofori 2016). In cases of mammary carcinomas, a population of the newly formed mesenchymal cells sustain a $CD44^{hi}CD24^{low}$ phenotype, which enables them to behave similarly to mesenchymal stem cells, enhances their metastatic and invasion potential and, eventually, leads to tumor cell dissemination (Lamouille, Xu et al. 2014, Chen, You et al. 2017).

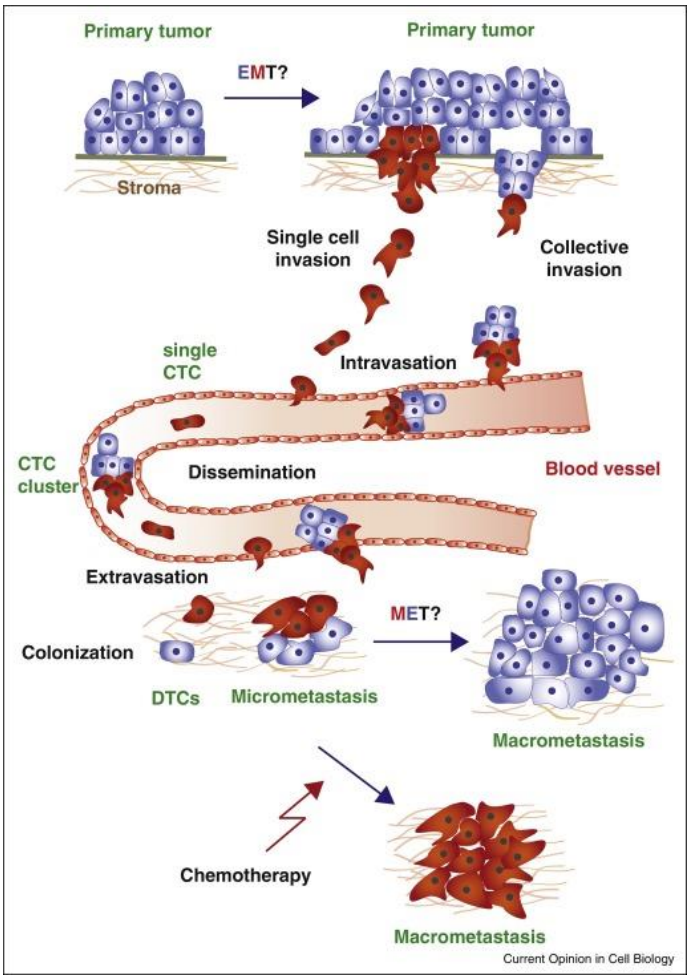

Figure 1.4: **Schematic representation of cancer cell metastasis**: Cancer cells exhibiting EMT are able for translocation into the blood circulation and dissemination through the vascular system. After extravasation cells can invade distant organs, form micro-metastasis, which eventually grows to macroscopic metastasis. CTC: circulating tumor cells, DTCs: disseminated tumor cells (Diepenbruck and Christofori 2016).

Aim of study

The function of PML in tumorigenesis is highly complexed due to the induction of opposite effects in distinct genetic/ epigenetic settings and cell types. We showed previously in our lab, that overexpression of PML IV isoform in TNBC MDA.MB.231 leads to cell growth arrest, accompanied by long-term survival and stress resistance signature, through activation of FOXO3 and inactivation of FOXM1 signaling (Sachini, Arampatzi et al. 2019).

To extend these studies we used here a loss of function approach to examine the role of PML knock down in breast cancer biology and in vivo tumorigenicity in immunocompromised mice. More specifically, we focused on cell proliferation and cell cycle progression, as well as invasion and metastatic ability of two breast cancer cell lines with distinct, mesenchymal or epithelial, features. Finally, we analyzed the gene expression profile of one of those and identified enriched cell growth and invasion deregulated gene sets.

2. Materials & Methods

2.1 Plasmids

For the generation of stable, knocked down cell lines, cells were infected by puromycin expressing lentiviral vectors carrying the relevant short hairpin (sh) sequences, followed by drug selection. The shPML plasmid used was kindly provided by Everett et al. (2006). The sequence for shPML was as follows: 5' AGATGCAGCTGTATCCAAGAAAGCCA 3'. Subcloning of the specific shPML into PLKO.1 vector was done via AgeI and EcoRI sites flanking the 5'-end of top and bottom shRNA oligo, respectively. mCherry LEGO-C was provided by addgene (#27348). Knockdown (KD) was evaluated by western and mRNA analysis using suitable primers.

2.2 Lentivirus production

Lentiviral vectors were obtained by HEK-293T transfection with calcium phosphate. Cells at 60% confluency were transfected with the corresponding vectors (20μg for 100mm dish), the packaging (12μg PAX for 100mm dish) and envelope (6μg PMD2G for 100mm dish). The next day the medium was changed and 72hr after transfection the supernatant was collected.

2.3 Cell culture

Human breast cancer cell lines MDA-MB-231 and MCF7 were cultured in DMEM, supplemented with 10% FBS and Gentamycin in 5% CO2 and at 37^{o}C. Tumourspheres were grown in DMEM-F12 1:1 (Gibco) medium containing B27 (1:50), bFGF (20ng/ml), EGF (20ng/ml) and 0.2% methylcellulose, in ultralow attachment plates.

2.4 RNA extraction

RNA was extracted using NucleoZOL reagent (Macherey-Nagel):

1. NucleoZOL (200 - 300μl depending the cell pellet) and dd H_20 (200 μl dd H_20 per 500 μl NucleoZOL) was added in cells
2. Vortex (15 sec) and centrifugation for 15 min, at 12000g (RT)
3. Equal volume of isopropanol (1:1) was added in the supernatant
4. Incubation for 10 min (RT) and centrifugation for 10 min, at 12000g (4^{o}C)
5. After drying the pellet 20μl of dd H_20 werer added and the RNA extracts were stored at -80 ^{o}C
6. Determination of RNA concentration by electrophoresis in 1.5% agarose gel, as well as by Nanodrop measurement.

2.5 Quantitative reverse transcription PCR (qRT-PCR)

2μg of RNA were used for reverse transcription to cDNA:

1. A mix was prepared with 2μg of RNA, dd H_20 (up to 11μl/sample), hexamers (1μl/sample) and dNTPs (1μl/sample)
2. Incubation for 5 min (65 ^oC)
3. B mix for each sample included 4μl 5x buffer (Minotech), 1μl 0.1M DTT, 0.2μl RT enzyme (Minotech) and 1.8μl dd H_20
4. Incubation for 60 min, at 42 ^oC
5. 20 μl of dd H_20 were added and cDNA was stored at -20 ^oC

Relative abundance of each transcript was measured by quantitative real time PCR using SYBR Green I. Relative mRNA expression was calculated after normalization against β-actin levels. Primer sets used for real qPCR analysis are:

PML	FW: 5'-CCCTGGATAACGTCTTTTTCG-3'
	RV: 5'-GGAGCTGCTCGCACTCAAAGC-3'
B – ACTIN	FW: 5'-CCTGTACGCCAACACAGTG-3'
	RV: 5'-ATACTCCTGCTTGCTGATCC-3'
BATF	FW: 5'-TGGCAAACAGGACTCATCTG-3'
	RV: 5'-CTGCTTGATCTCCTTGCGTA-3'
FASCN1	FW:5'-CAGCGGCCTCTCGTCTA-3'
	RV:5'-AGATCTGCTTCTTCTTCAGGC-3'
ICAM1	FW: 5'-ACCCTGTCAGTCCGGAAATA-3'
	RV: 5'-AGGATGACTTTTGAGGGGGA-3'
PIM1	FW:5'-CGAGCATGACGAAGAGATCA-3'
	RV: 5'-TCGGGCATCTGACAAGAGA-3'
MMP1	FW: 5'-GGGCTTTGATGTACCCTAGC-3'
	RV: 5'-GCTCAACTTCCGGGTAGAAG-3'
IL6 – ST	FW: 5'-CGAAGCTGTCTTAGAGTGGG-3'
	RV: 5'-AAGCAAACAGGCACGACTAT-3'
CD49f	FW: 5'-TCATGGATCTGCAAATGGAA-3'
	RV: 5'-AGGGAACCAACAGCAACATC-3'
CDH1	FW: 5'-CTGACACACCCCCTGTTGGT-3'
	RV: 5'-GTGAATTCGGGCTTGTTGTC-3'
SLIT2	FW: 5'-ACCAGTCATTTATGGCTCCTTC-3'
	RV: 5'-TCAGAGAGCGTAGTCCTTGG-3'
PCNA	FW: 5'-TTTCCTGTGCAAAAGACGGA-3'
	RV: 5'-CCGTTGAAGAGAGTGGAGTGG-3'
TOP2A	FW: 5'-TCAAACGGAATGACAAGCGA-3'
	RV: 5'-ATGGGCTGCAAGAGGTTTAG-3'
NLRP1	FW: 5'-GAACTGGAGCTCTGCTATCG-3'

	RV: 5'-ATCCAGAGGTGAAGGTACGG-3'
IL6	FW: 5'-ACTGGCAGAAAACAACCTGA-3'
	RV: 5'-CAGGGGTGGTTATTGCATCT-3'
HDAC9	FW: 5'-GGTGGACAGTGACACCATTT-3'
	RV: 5'-TGGATTCTTCAGCGTGATGG-3'

2.6 Protein extraction

Proteins were extracted with RIPA buffer (25 mM Tris pH 7.6, 150 mM NaCl, 1% NP-40, 1% Deoxycholate, 0.1% SDS, 1 mM PMSF):

1. 60 - 80 μl of RIPA with protease and phosphatase inhibitors were added in the cell pellet
2. Incubation for 30 min (ice) and centrifugation for 20 min, at 14000rpm (4 ^{o}C)
3. Determination of protein concentration by Bradford assay.

2.7 Western blot

4. Equal amounts of protein extract were subjected to SDS – PAGE electrophoresis
5. Gel was transferred to a 0.45μm PVDF membrane and blocked for 1hr with 5% BSA
6. Incubation with primary antibody solution (in 2.5% BSA) for 1hr RT or overnight in 4 ^{o}C
7. Washes with TBS-T and incubation with secondary antibody solution (1:10000 in 5% milk) for 1hr
8. Chemiluminescent detection with the ECL method (Thermo Scientific)

Primary antibodies used for western blotting are:

β-ACTIN (sc-47778, Santa Cruz), PML (sc-377340, Santa Cruz), ZEB1 (sc-25388, Santa Cruz), VIMENTIN (5741S, Cell signaling), CDH1 (3195S, Cell signaling), B – CATENIN (sc-7963, Santa Cruz).

2.8 Cell cycle analysis

For cell cycle analysis, 100.000 cells from each sample were trypsinized, washed with PBS, treated with RNAse A for 30 min at 37^{o}C and stained with propidium iodide (PI-Sigma) according to the manufacturer's protocol. The analysis was conducted using a FACS Calibur analyser. The cell cycle profile was further analysed using the ModFit LT software.

2.9 Invasion assay

2000 cells were cultured in non-adherent plates with DMEM + 2% BME (Cultrex® RGF BME Type 2) in order to form spheres:

1. Individual spheres, with a size > 100μm, were transferred to a U-bottom plate
2. Each U-bottom plate contained three layers of culture media:

1st layer: 50μl BME, incubated for 30min, at 37°C (5% CO_2)

2nd layer: ~50μl DMEM + 10% FBS: BME (1:1)

3. One sphere was transferred per well into the 2nd layer
4. Centrifugation for 5 min, at 500rpm (4°C) and incubation for 30min, at 37°C (5% CO_2)
5. Addition of 100μl warm DMEM + 10% FBS (3rd layer)

Invasion of cells was observed for 9 days after U-bottom plated spheres acquired a compact formation.

2.10 Flow cytometry

1. Collection of the cells in suspension and centrifugation for 10 min, at 400g
2. Addition of 1ml cold PBS/well and incubation for 15 min, at 4°C
3. Addition of the cells in suspension to the pellet in each tube
4. Centrifugation for 10 min, at 400g
5. The PBS was discarded and conjugated primary antibodies diluted in 3% PBS-FBS, 0.1% NaN3 were added
6. Incubation for 20 min at 4°C
7. Resuspention in 400μl PBS-FBS and centrifugation for 10 min at 400g

Primary antibody used: CD44 (PerCP/Cy5.5, Biolegend).

2.11 RNA – Sequencing

RNA-Seq was done by the 3'QUANTseq approach using the Ion Torrent technology (IMBB genomics facility). Data were mapped to hg19 with HISAT2 (ref to mapper https://www.nature.com/articles/nmeth.3317). Analysis was done by Cuffdiff (https://www.nature.com/articles/nprot.2012.016) and Metaseqr, count based analysis that combines different algorithms (https://academic.oup.com/nar/article/43/4/e25/2411004). DEGs were identified at a 1.5 or 2 fold change level and FDR<0.05.

2.12 ChIP – Sequencing analysis

PML genome binding/occupancy profiling by high throughput sequencing in MCF7 cells was downloaded from ENCODE Data Coordination Center (DCC: ENCSR155VDK, GEO: GSE95952), released from Richard Myers laboratory.

2.13 Statistical analysis

Statistics were determined using the Microsoft Excel 2010 or RStudio programming language, Version 1.1.453. Values were presented as the mean +SD.

2.14 Animals

Non-obese diabetic severe combined immunodeficient gamma (NSG) mice were subcutaneously injected with control and PML KD MDA.MB.231 and MCF7 cells. All lines were tagged by an mCherry lentivirus. Four groups of mice arose: two groups of five mice each, injected with 100.000 MDA.MB.231 control and KD cells respectively, one group of seven mice, five females and two males, injected with 400.000 MCF7 control cells and one group of 8 mice, six females and two males injected with 400.000 MCF7 PML KD cells. The tumor volume was measured for approximately two months post injection, according to the type of ellipsoid volume: $\frac{\pi}{6} * (major\ axis * minor\ axis * vertical\ axis)$. Estradiol was administrated orally, in drinking water to MCF7 injected female mice.

2.15 Ethical Approval for the Use of Animals

The NSG mice were purchased from Jackson Laboratory. All experiments were conducted in accordance with the Laboratory Animal Care and Ethics Committee of FORTH and approved by the regional animal well fare directorate (ΑΔΑ Ω5Π67ΛΚ-Μ41).

3. Results

3.1 PML affects the expression of cell cycle and cell adhesion related genes in breast cancer cells

In order to identify the involvement of PML in breast cancer, PML knock down was performed in two breast cancer cell lines: the claudin – low, triple – negative and aggressive MDA.MB.231 and the luminal A type, PR^+/ ER^+/ $HER2^-$ MCF7. PML was stably silenced in both cell lines, as evaluated in mRNA and protein level by qPCR and western blot analysis, respectively (Figure 3.1).

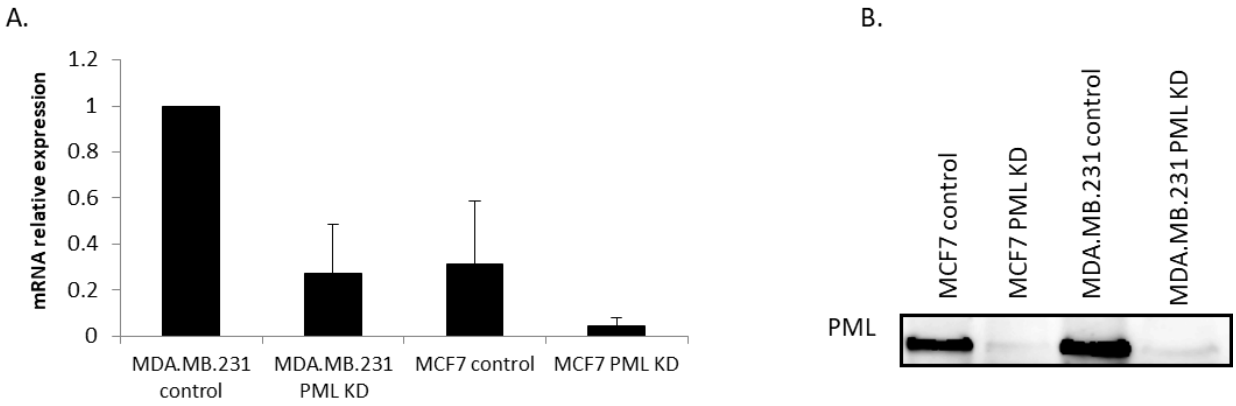

Figure 3.1: **PML KD in MDA.MB.231 and MCF7 breast cancer cell lines.** A. Relative mRNA levels (fold change) of PML in control and PML KD breast cancer cell lines. Error bars indicate +SD in three independent experiments (n=3). B. PML protein levels of control and PML KD cells. β-actin was used as a loading control.

Initially, we analyzed the transcription profile of MDA.MB.231 control and PML KD cells, from genome – wide expression sequencing performed previously in the lab. Using a p-value ≤ 0.05 and fold change cut off of 1.5, the RNA – Seq revealed 1041 differentially expressed genes in the PML KD state, while 577 of them were over-expressed and 464 were under-expressed, as shown in Figure 3.2A. Selected genes implicated in different biological processes (cell cycle, DNA replication, cell adhesion, chromatin modification, migration and immune response) were validated by qPCR. As expected, PML was downregulated along with genes related to cell adhesion, such as E – Cadherin, Integrin A6 (CD49f) and ICAM1, accompanied with repression of genes related to immune response (IL6 and the receptor, IL6-ST) and the chromatin modifier HDAC9. In contrast, selected genes related to DNA replication, proliferation and motility were up-regulated (Figure 3.2B, 3.2C).

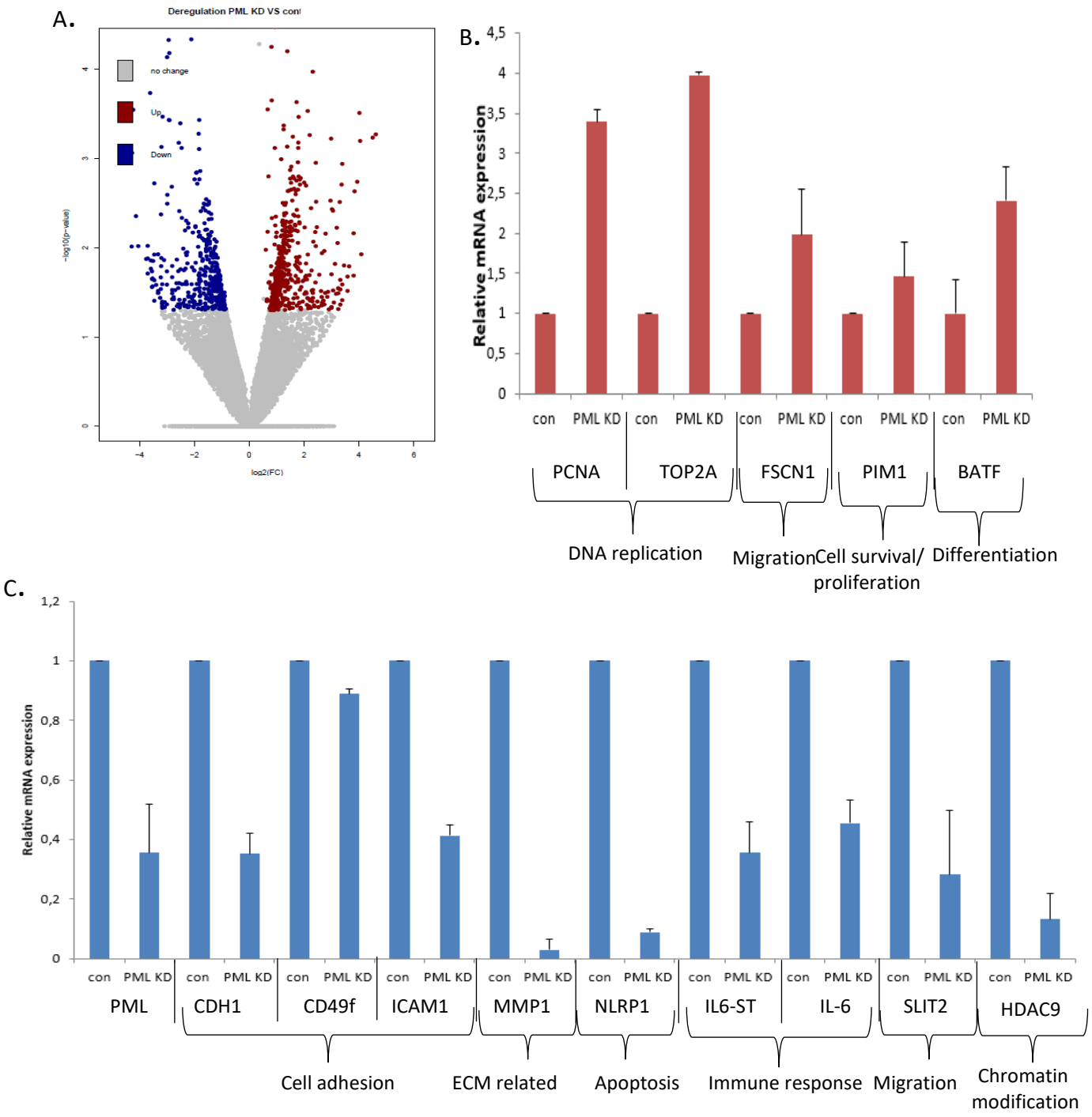

Figure 3.2: **Changes of global gene expression upon PML KD in MDA.MB.231 cell line.** A. Volcano plot depicting the distribution of differentially expressed genes after PML KD (fold change>1.5, p≤0.05). B. Validation of RNA -Seq. Relative mRNA levels (fold change) of selected over - expressed genes upon PML KD. C. Relative mRNA levels (fold change) of selected under - expressed genes upon PML KD. Error bars indicate +SD of three independent experiments (n=3).

The list of differentially expressed genes was further analyzed using the g:Profiler software. Biological process (BP) and KEGG pathway functional analysis demonstrated that upon PML KD, up-regulated genes were enriched in processes related to cell cycle, mitosis, cell division, as well as proteasome, ribosome and oxidative phosphorylation pathways. On the other hand, down-regulated genes were over-represented in cell adhesion, developmental process, cellular senescence and FoxO signaling pathway (Figure 3.3).

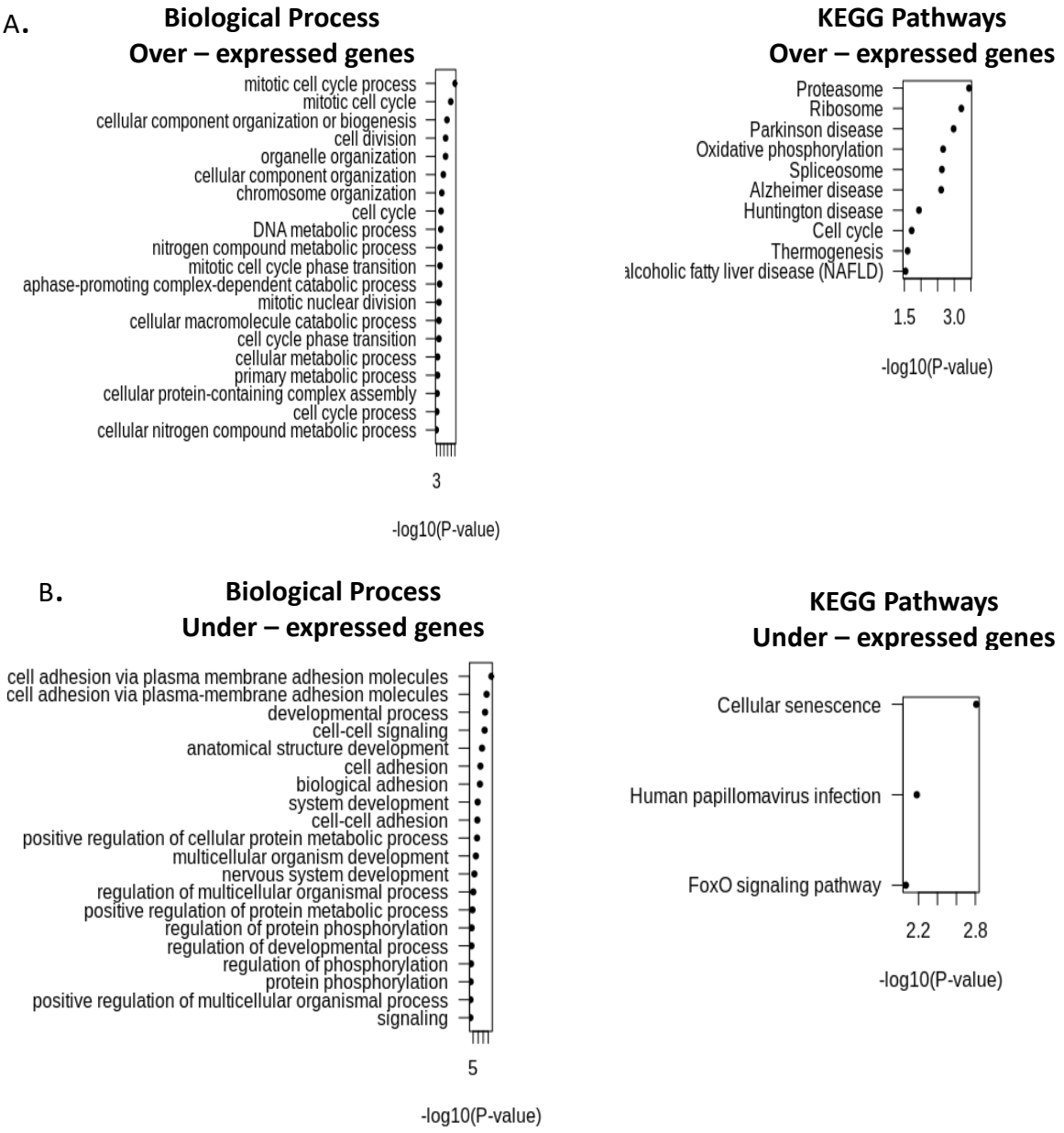

Figure 3.3: **Functional enrichment analysis of differentially expressed genes upon PML KD in MDA.MB.231.** A. Up-regulated genes. B. Down-regulated genes. Functional analysis performed using g:Profiler. Scatter plots show significantly enriched Biological process (GO:BP) in the left panel and KEGG pathways in the right panel.

3.2 PML represses the expression of genes related with cell cycle

Subsequently, we wanted to investigate genes whose expression is closely related to PML binding. For that reason, we downloaded a publicly available from the ENCODE project chromatin immunoprecipitation - DNA sequencing (ChIP –Seq) experiment and we detected DNA regions associated with PML in MCF7 cells. We matched the 4814 PML peaks from the ChIP – Seq to 3177 genes using the human reference genome GRCh37 (hg19) from the Reference Sequence (RefSeq) database and we extended each one by 3000bp upstream and downstream. We next divided each gene in 6 regions: the four quarters of the gene and the parts from 3000bp upstream till the transcription start site and from the transcription end site until 3000bp downstream. The list of PML target genes was further classified by silhouette clustering into five clusters, depending on the region they were bound by PML. Out of 3177 genes bound by PML, 1683 were bound in the first two parts, that is 3000bp upstream till the first quarter of the gene (red cluster), 223 were bound either in the first or the second quarter (yellow cluster), 302 were bound exclusively in the upstream region (blue cluster), while 498 in the downstream region (green cluster) and the last cluster (purple) contained 471 genes bound widely by PML (Figure 3.4A).

The next step was to detect which of the genes bound by PML were deregulated after PML silencing. We tested all the possible overlaps between each cluster and the differentially expressed genes and by permutation test we found statistically significant overlap only between the up – regulated genes and the red cluster (enrichment 2.09, p-value 0), as well as the purple cluster (enrichment 2.16, p-value 0.002) (Table 3.1). We further investigated the overlap between the 577 over – expressed genes and the 1683 genes of the red cluster, which demonstrated 62 genes enriched among others in cell cycle and mitotic processes (Figure 3.4B, 3.4C).

Clusters		Up – regulated genes	Down – regulated genes
Red	Enrichment	2.0982808	0.6558299
	P - value	0.0000000	0.9420000
Yellow	Enrichment	0.4948046	1.7507003
	P - value	0.7510000	0.0650000
Purple	Enrichment	2.1652833	1.3061224
	P - value	0.0020000	0.1600000
Blue	Enrichment	0.7371913	2.1058173
	P - value	0.6280000	0.0140000
Green	Enrichment	1.2358162	1.0894942
	P - value	0.1760000	0.3030000

Table 3.1: **Matrix of the overlaps between differentially expressed genes and PML binding clusters**. Statistical significance was calculated by permutation test.

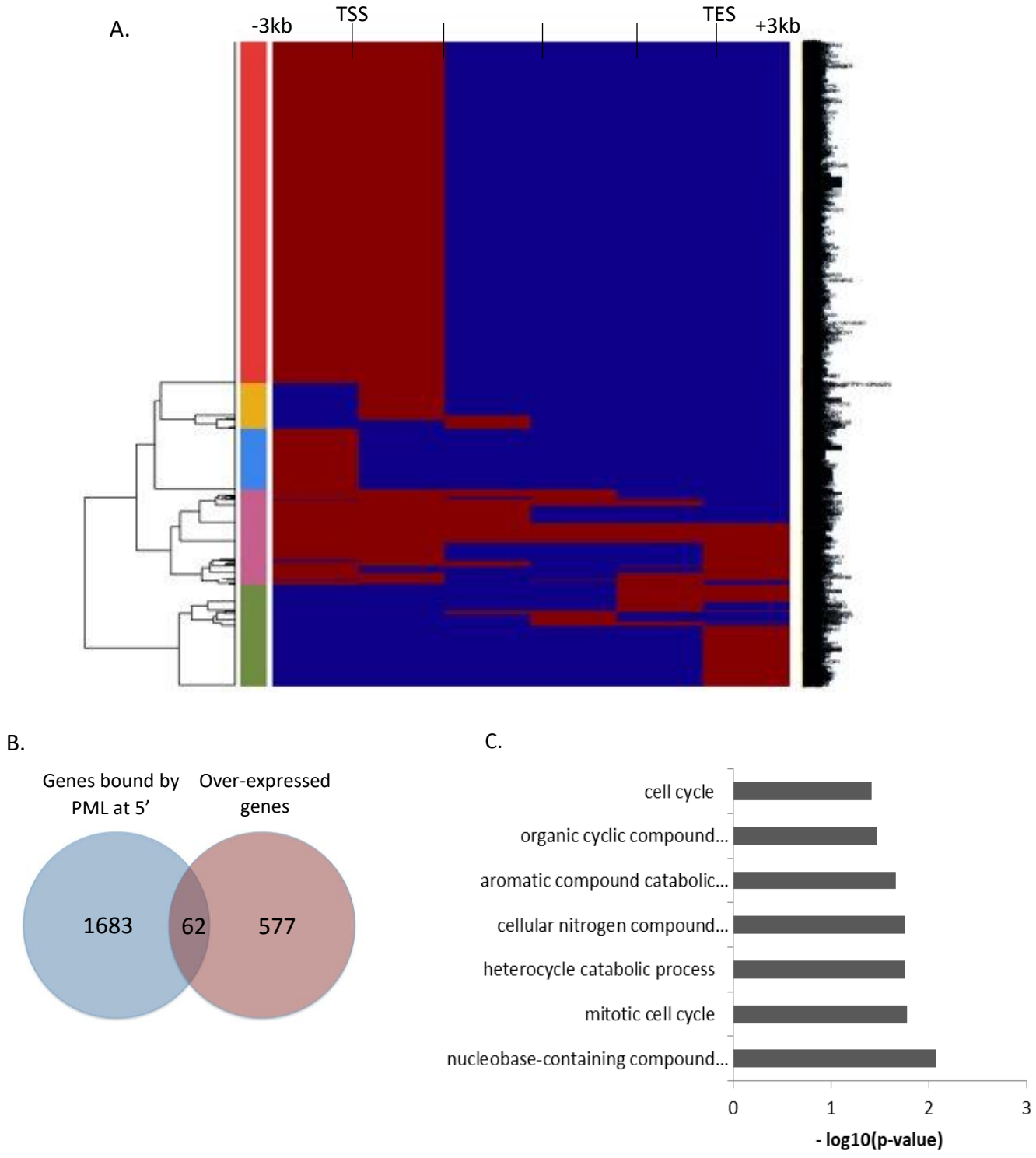

Figure 3.4: **PML binding pattern analysis**. A. 3177 genes bound by PML are categorized into five clusters by Silhouette clustering, according to PML binding. Dark red color represents the gene regions bound by PML and dark blue color represents PML free regions. B. 62 genes overlap with statistical significance between the differentially expressed genes upon PML KD in MDA.MB.231 cells and the genes bound by PML in MCF7 cells. C. Functional enrichment of the 62 overlapping genes, using g:Profiler.

To further understand the role of PML in cell proliferation we examined whether the proliferation rate of PML KD cells differed from the control cells. As shown in Figure 3.5, MDA.MB.231 seemed to proliferate slower in the KD state, whereas MCF7 exhibited increased proliferation capacity upon PML KD (Figure 3.5A, 3.5B). Additionally, we assessed the impact of PML KD on cell cycle progression. In both cell types, the PML KD state displayed a slight increase in cell fractions in the S phase together with a reduction in G1 phase, whereas G2 was not affected (Figure 3.5C).

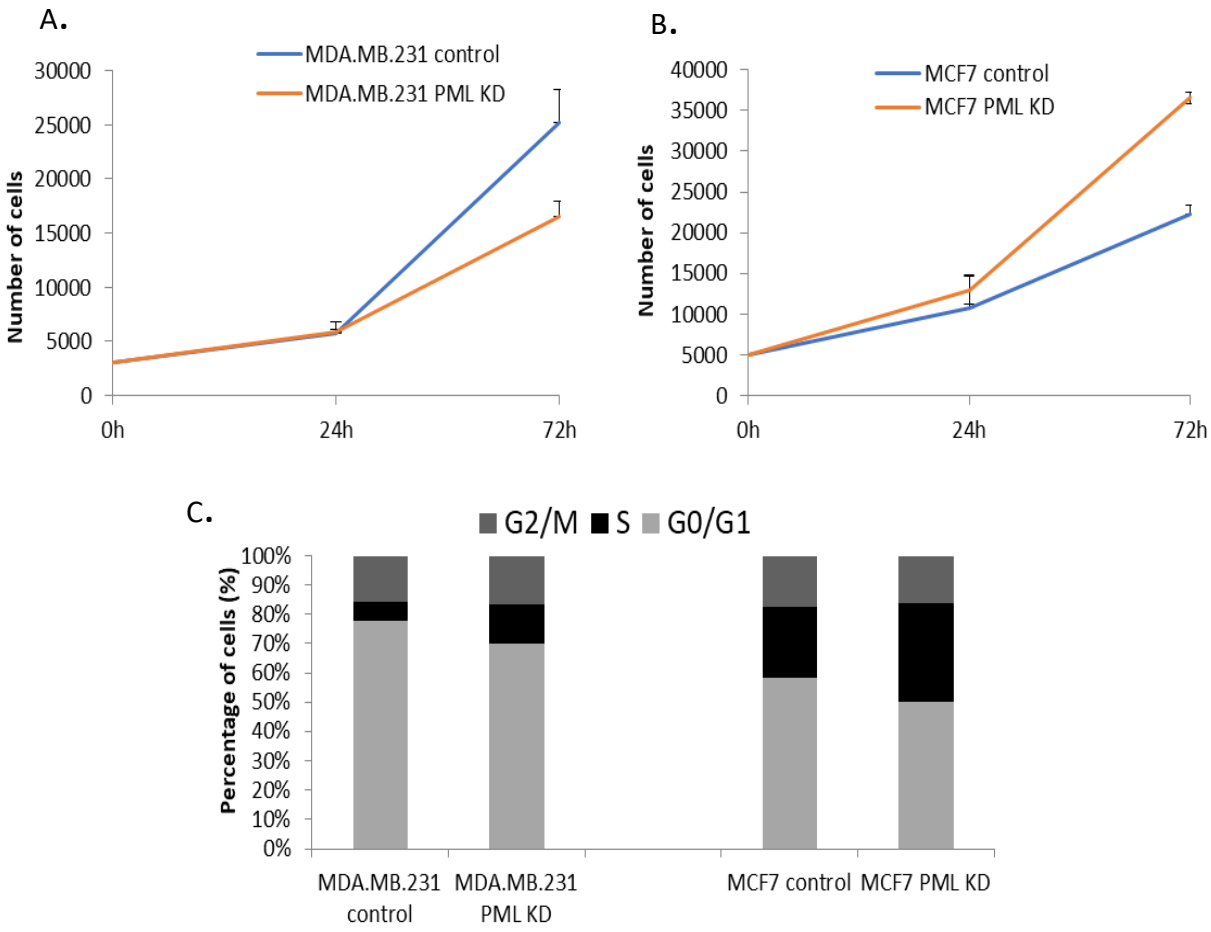

Figure 3.5: **Proliferation rate and cell cycle progression of MDA.MB.231 and MCF7 cells upon PML KD**. A. Cell growth of control and PML KD MDA.MB.231 cells. B. Cell growth of control and PML KD MCF7 cells. Data represent the mean +SD of three independent experiments (n=3). C. Cell cycle analysis of control and PML KD MDA.MD.231 and MCF7 cells stained with propidium iodide (PI) and analyzed using flow cytometry.

3.3 PML KD induces EMT in MCF7 cells and enhances aggressiveness in MDA.MB.231 cells

We next examined the morphology of cells cultured in monolayer or in three-dimensional culture system. We observed small morphological differences between control and PML KD MDA.MB.231 cells in both 2D and 3D culture models. MCF7 cells however, exhibited a profound change upon PML KD. While control cells tend to form an epithelial layer of tightly connected to each other cells through adherens, tight and gap junctions, PML KD MCF7 seemed to lose the cell to cell adhesion ability. In agreement, MCF7 control tumor spheroids are round – shaped, surrounded by epithelial layers and empty inside possibly due to cell anoiikis, whereas MCF7 PML KD spheres appeared to be similar to the MDA.MB.231 ones (Figure 3.6).

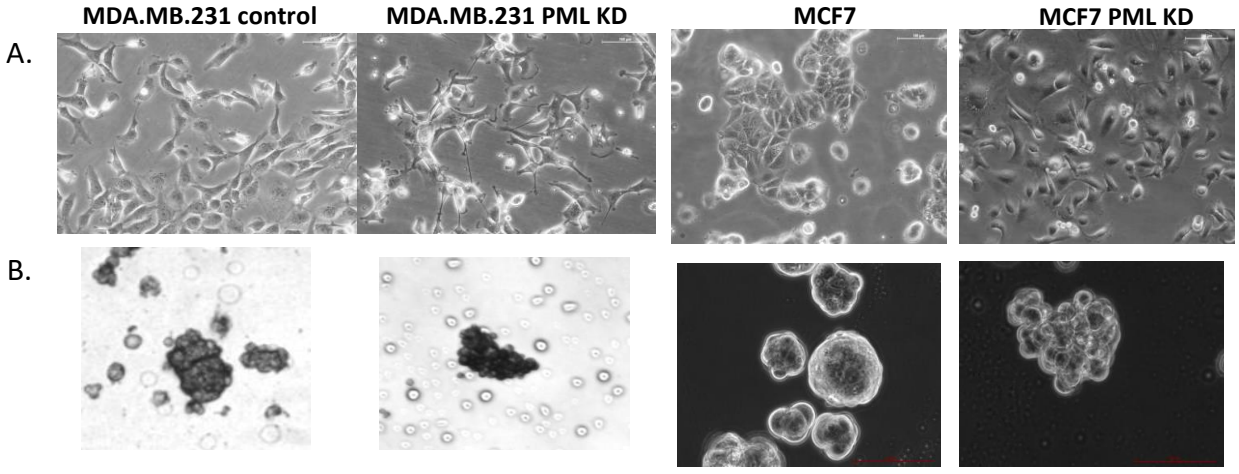

Figure 3.6: **Monolayer and three dimensional cultures of MDA.MB.231 and MCF7 cells.** A. 2D culture of breast cancer cells in control and PML KD state. B. Tumorsphere formation of control and PML KD cells cultured in non – adherent plates.

To further understand the role of PML in breast cancer we performed an invasion assay. PML KD seemed to enhance the invasion capacity in both cell types, in comparison with the control cells (Figure 3.7). The difference was apparent between MCF7 control and KD cells, as invasion stared earlier in the case of PML KD, leading to a disperse morphology of the sphere at the end of the assay.

A. **MDA.MB.231 control**

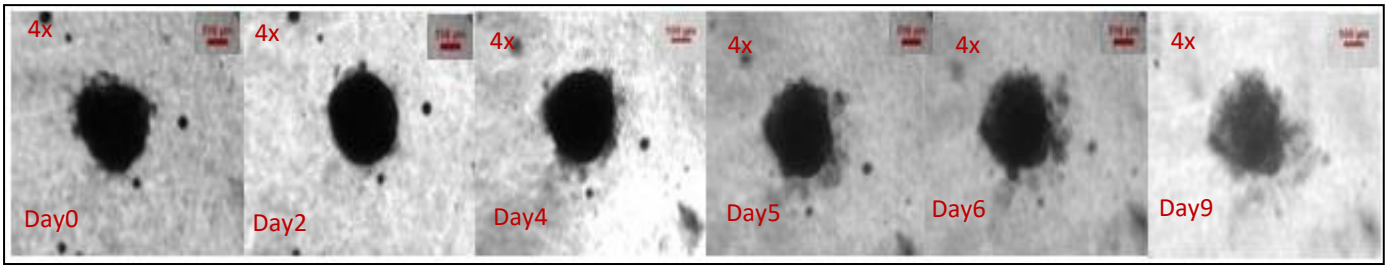

MDA.MB.231 PML KD

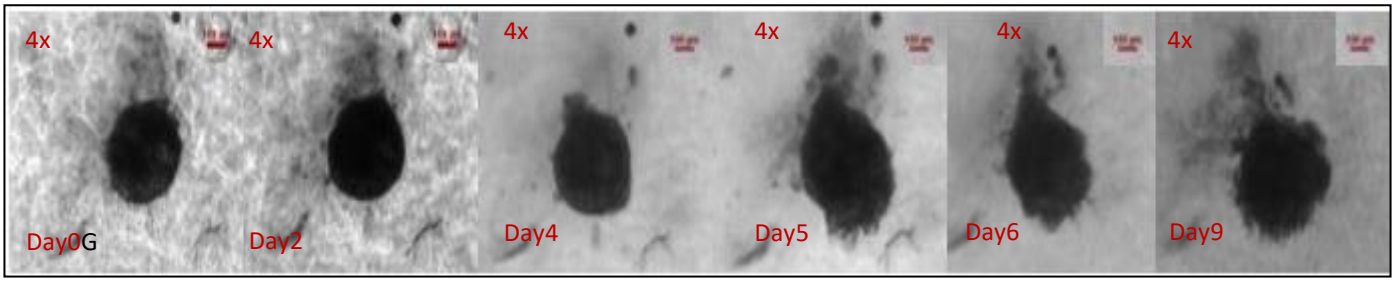

B. **MCF7 control**

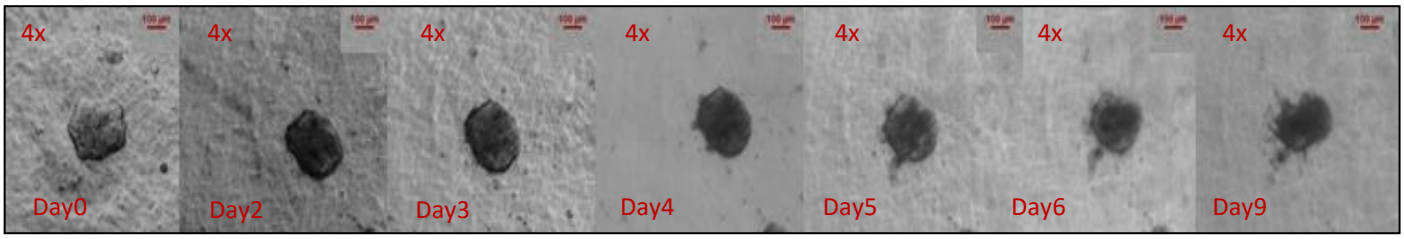

MCF7 PML KD

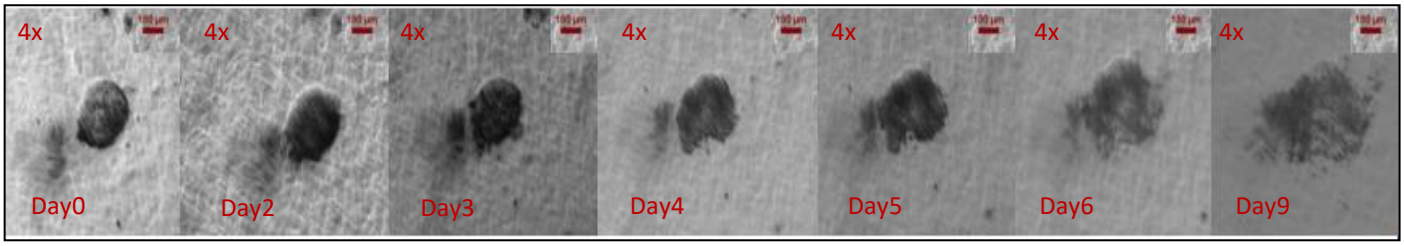

Figure 3.7: **Invasion capability of MDA.MB.231 and MCF7 cells**: A. Invasion of control and PML KD MDA.MB.231 cells. B. Invasion of control and PML KD MCF7 cells. Individual tumorspheres are placed in well plates containing matrigel.

In order to further investigate the loss of epithelial characteristics of MCF7 cells upon PML KD, we evaluated specific EMT related markers by western blot and flow cytometry. We detected induction of the mesenchymal markers Vimentin and Zeb1, stably expressed in MDA.MB.231 but absent in MCF7 control cells, whereas E-cadherin and B-catenin, two epithelial markers, were slightly reduced in MCF7 PML KD cells (Figure 3.8A). The mesenchymal transduction is also enhanced by the observation that PML KD MCF7 started expressing the mesenchymal marker CD44, as indicated by flow cytometry (Figure 3.8B).

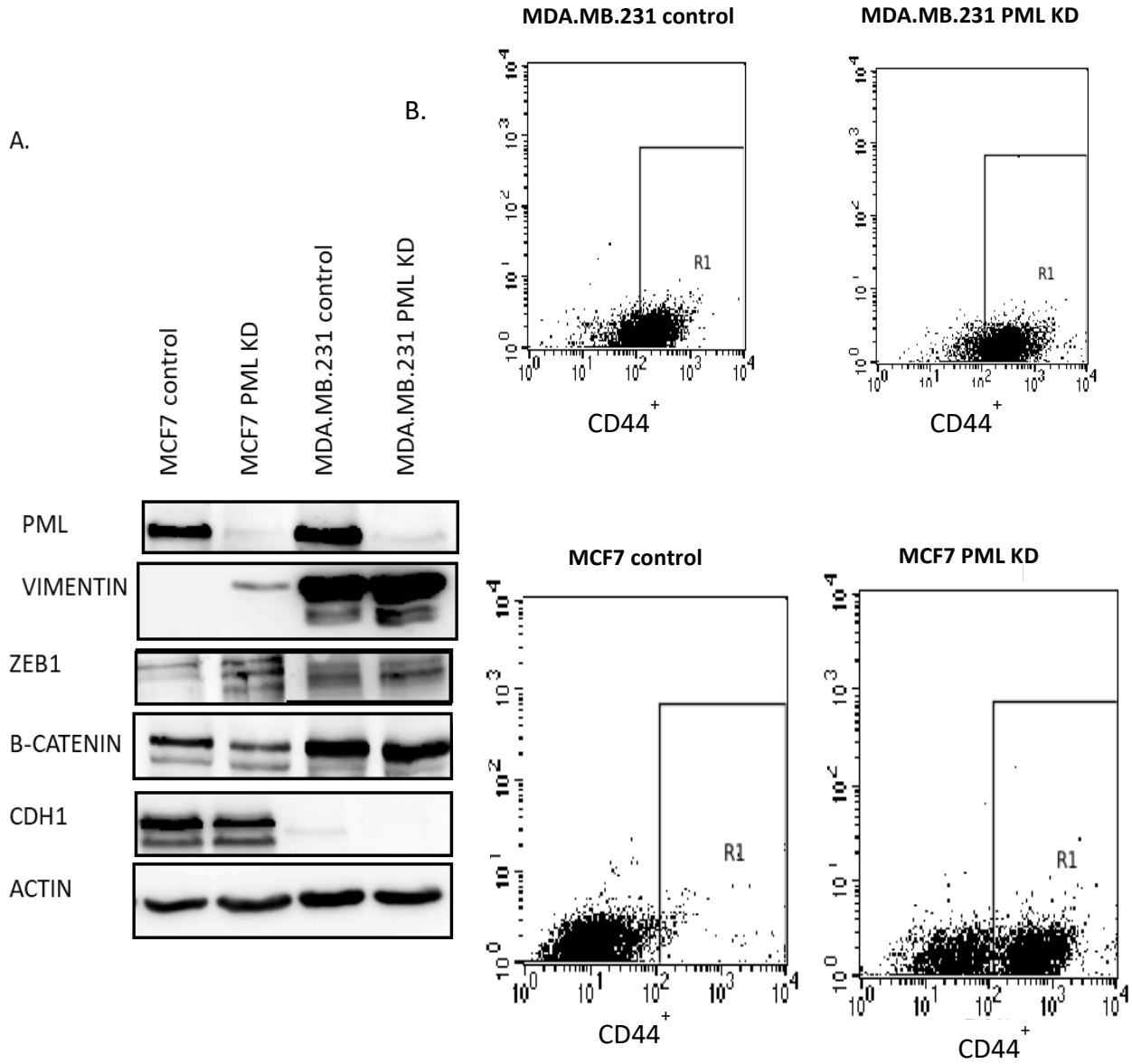

Figure 3.8: **Changes in the expression of epithelial-mesenchymal related markers**: A. Western blot analysis of epithelial (E-cadherin, B-catenin) and mesenchymal (Vimentin, Zeb1) markers in control and PML KD MDA.MB.231 and MCF7 cells. β-actin was used as a loading control. B. Flow cytometry dot plot of CD44 mesenchymal marker in control and PML KD MDA.MB.231 and MCF7 cells.

3.4 PML KD enhances tumor growth and metastatic ability in both MDA.MB.231 and MCF7 cells

The following step was to investigate the effect of PML KD *in vivo* (Table 3.2). All mice injected with MDA.MB.231 cells, control and KD, formed tumor 17 days after injection. The KD group showed a slightly faster tendency, as three out of five mice had already formed tumors two weeks post injection, whereas in the same time only one MDA.MB.231 control injected mouse appeared to develop tumor. MCF7 injected mice displayed similar tumor growth rates during the first month, however PML KD MCF7 grew faster, leading to tumor development of all individuals 32 days post injection, while the same happened 11 days later in the case of MCF7 control group (Figure 3.9). As far as the tumor size, in both cell types the control groups formed smaller tumors, as demonstrated in figure 3.10.

Cell line	**MDA.MB.231**		**MCF7**	
Injected mice	Control: 5	PML KD: 5	Control: 7	PML KD: 8
Sex	males	males	5 females 2 males	6 females 2 males
Number of injected cells/ animal	100.000	100.000	400.000	400.000
Experiment duration (weeks)	6	6	7	7
Estradiol administration	No	No	Yes (female)	Yes (female)
Metastases	Liver (5/5) Lung (5/5) Lymph (axillary) (4/5) Kidney (1/5)	Liver (3/4) Lung (4/4) Lymph (axillary) (4/4) Kidney (3/4) Femoral bone (2/4)	Lung (5/7) Lymph (intestinal) (4/7) Ascites (5/7) Ovary (2/7)	Liver (7/7) Lung (7/7) Lymph (axillary) (5/7) Kidney (3/7) Ureter (2/7) Femoral bone(1/7)

Table 3.2: **Recapitulation of the *in vivo* experimental setup**. Four groups of injected mice were tested, regarding their ability to form tumors and metastasize to distant organs. One mouse with tumor died in the KD group without being evaluated.

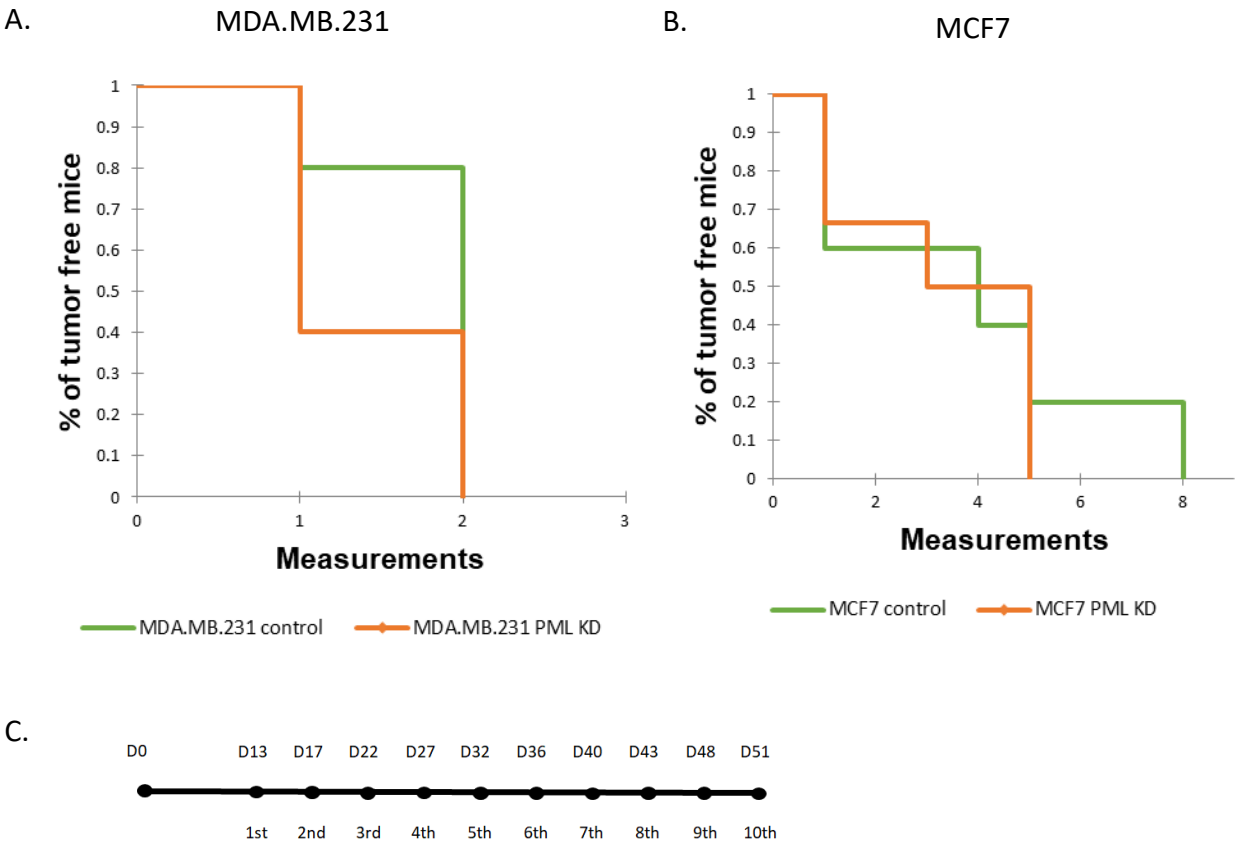

Figure 3.9: **Frequency of primary tumor formation**. Kaplan Meier probability plots for disease incidence of the injected with control and PML KD MDA.MB.231 cells (A) and control and PML KD MCF cells (B). C. Time table of mouse follow up from the day of injection (Day 0).

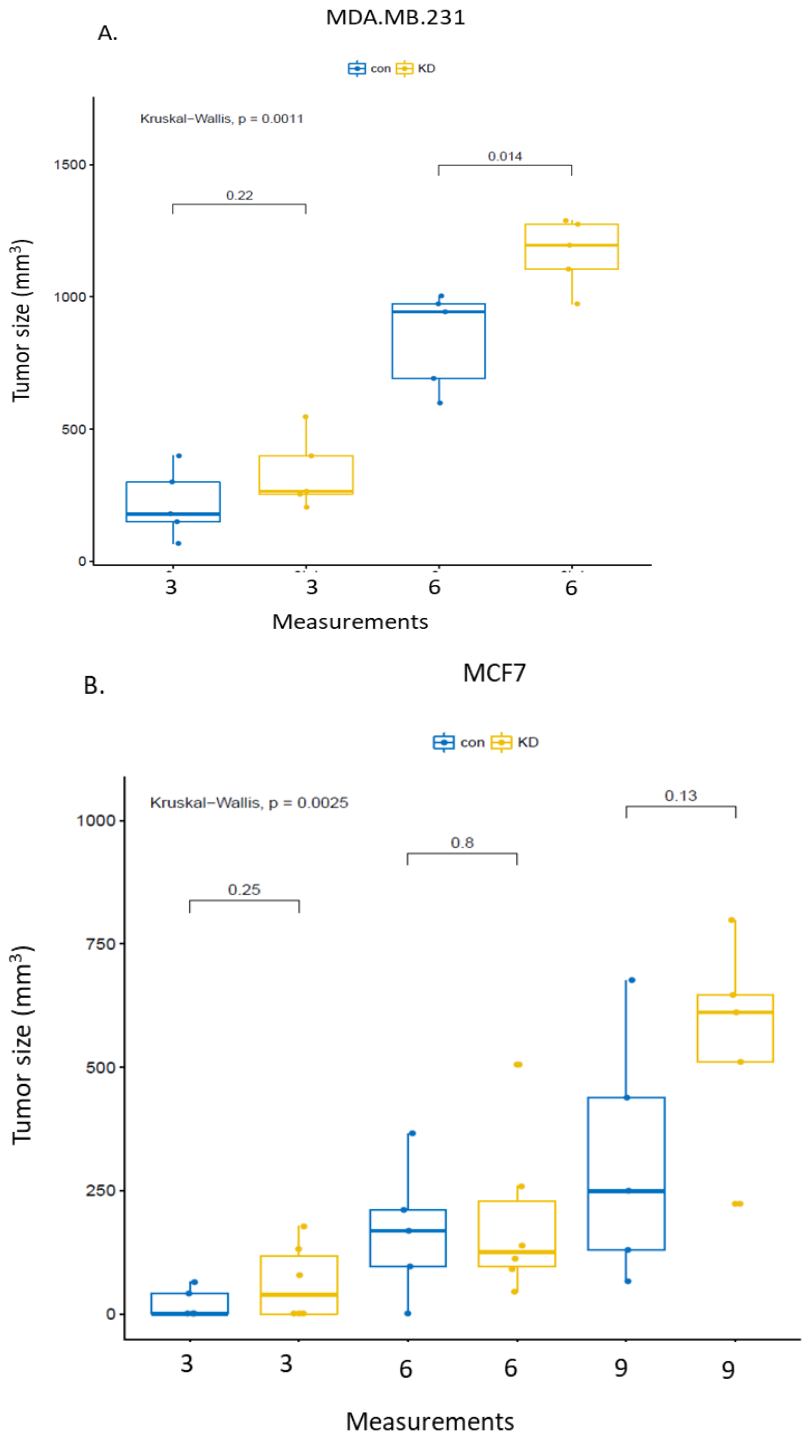

Figure 3.10: **Boxplots of tumor volume in different time points**: A. Comparison of tumor volumes of MDA.MB.231 control and PML KD injected mice in two time points. B. Comparison of tumor volume of MCF7 control and PML KD injected mice in three time points. Measurement 3 = Day 22, Measurement 6 = Day 36 and Measurement 9 = Day 48.

Finally, we evaluated the metastatic ability of the two cell lines. As expected, the aggressive MDA.MB.231 cells displayed elevated metastatic potential in contrast to MCF7 cells. Both control and PML KD MDA.MB.231 migrated mainly to the lung, the liver and the proximal (axillary) or distant lymph nodes, although more metastatic foci were found in KD cells. On the other hand, the metastatic ability of MCF7 control cells was decreased comparing to KD cells, which agrees with the notion that upon PML KD, MCF7 cells lose their epithelial character and increase their motility, as represented in Figure 3.11.

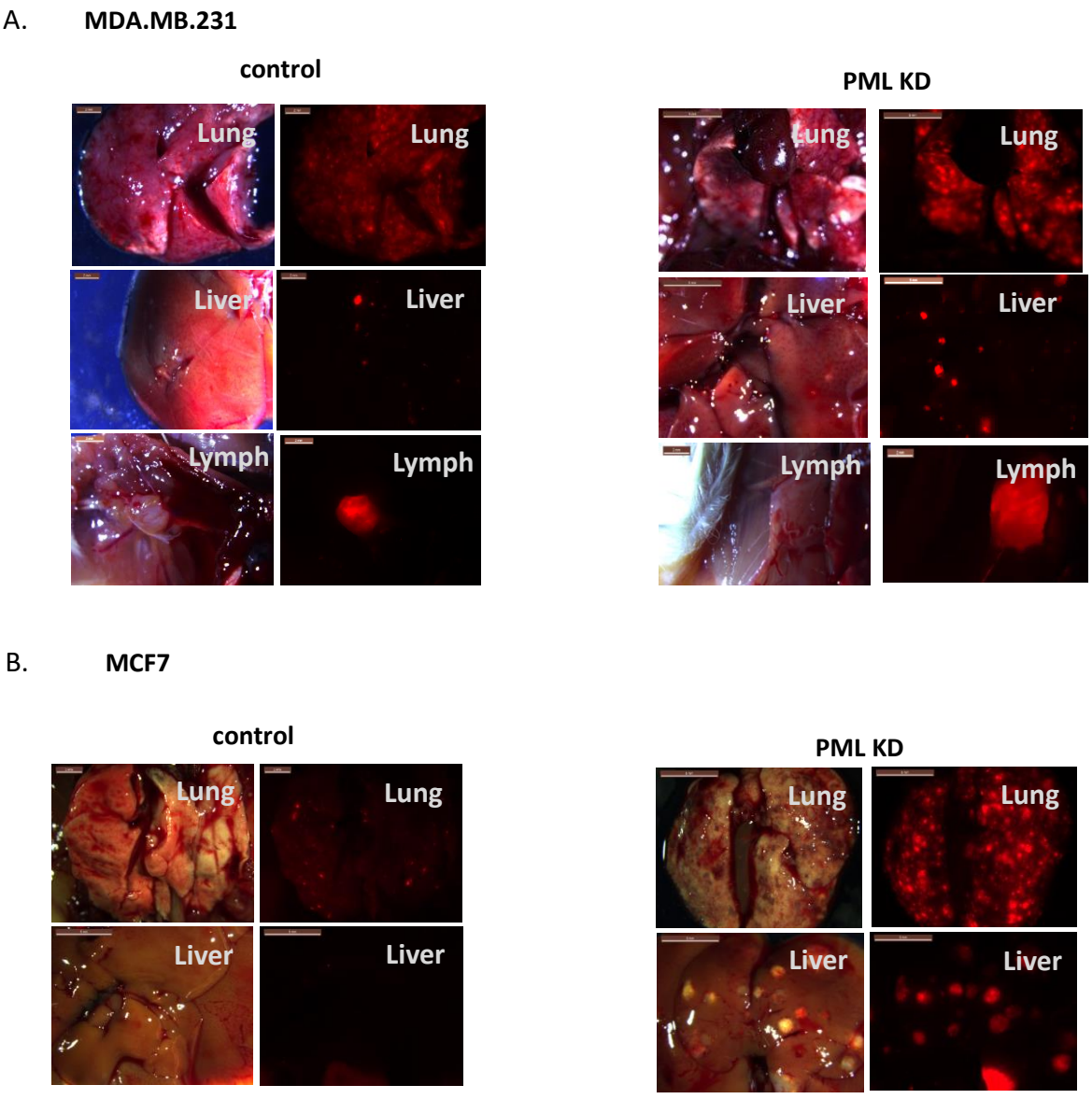

Figure 3.11: **Metastatic foci in lung, liver and lymph**: A. Comparison of the metastatic ability of control and PML KD MDA.MB.231 cells, injected in mice. B. Comparison of the metastatic ability of control and PML KD MCF7 cells, injected in mice. Left panels: visible light. Right panels: red fluorescence (mCherry).

4. Discussion

Having in mind that overexpression of the PML IV isoform arrests cell growth in MDA.MB.231 (Sachini, Arampatzi et al. 2019), we wanted to monitor the effect of PML KD in two breast cancer cell lines, MDA.MB.231 and MCF7. We, initially, detected differentially expressed genes upon PML silencing, showing that the list of over – expressed genes is enriched in cell cycle related processes. Although the transcription profile analysis was accomplished in the aggressive, triple – negative MDA.MB.231 cell line, we compared the data with a ChIP – Seq prepared in the luminal A, epithelial MCF7 cells. Among others, the ChIP – Seq analysis demonstrated 62 statistically significant overlapping genes between the two breast cancer cell lines. These genes are bound by PML in the upstream region, while in the absence of the protein they are over – expressed, implying that PML suppresses their expression. Apparently, PML is implicated in processes related to cell proliferation and cell cycle progression. Specifically, PML KD seems to slightly enhance the proliferation and cell cycle in MCF7 cells, whereas the effect in MDA.MB231 is ambiguous.

Although we cannot come to a conclusion regarding PML's involvement in cell cycle, our observations about the epithelial to mesenchymal transition in the lack of PML are more prominent. Based on the first notion that the expression of genes related to cell to cell adhesion pathways is reduced when PML is missing in MDA.MB.231 cells, we examined whether the aggressiveness of this type of breast cancer cell line is enhanced upon PML KD. Indeed, PML KD cells displayed a higher tendency to invade, an increased metastatic ability and formed greater primary tumors in contrast to the control group of mice.

A similar set up of experiments, performed in MCF7 cells, pointed out a loss in their epithelial signature in the absence of PML. Interestingly, PML KD MCF7 cells' behavior seemed relevant to the mesenchymal MDA.MB.231 cell line in terms of morphology, invasion and metastatic potential. MCF7 cells cultured in a monolayer appeared to lose the cell to cell adhesion ability, whereas they formed tumor spheres missing the compact morphology shown in control cells. Furthermore, it was evident that the invasion capacity, as well as the metastatic ability was increased upon PML KD. The group of PML KD MCF7 injected mice showed a greater number of metastatic foci in a plethora of organs, compared to the control group. In addition, the PML KD group of mice tended to form tumors with a greater volume in contrast to the control MCF7 injected mice; however both control and KD MCF7 are smaller than the tumors formed by MDA.MB.231 at the same time. Finally, another interesting observation was that both male mice injected with PML KD MCF7 cells were capable to form tumors without estradiol administration. This might attribute one more possible feature in PML's function, regarding the overcome of estrogen receptor mediated signaling in tumorigenesis.

In conclusion, we investigated the involvement of PML in cell cycle progression, epithelial – mesenchymal transition and tumorigenesis in breast cancer cell lines. The results point out to a possible implication of PML in the maintenance of epithelial characteristics and the restriction of tumor aggressiveness. Further experiments are needed to clarify the transcriptional and post transcriptional mechanisms involved.

5. References

A. Kakizuka, W. H. M., Jr.,t K. Umesono, R. P. Warrell, Jr.,5 S. Ft. Frankel, V. S. Murty,E. Dmitrovsky, and R. M. Evans (1991). "Chromosomal Translocation t(l5;17) in Human Acute Promyelocytic Leukemia Fuses RARa with a Novel Putative Transcription Factor, PML." Cell **66**.

Bernardi, R. and P. P. Pandolfi (2007). "Structure, dynamics and functions of promyelocytic leukaemia nuclear bodies." Nat Rev Mol Cell Biol **8**(12): 1006-1016.

Bill, R. and G. Christofori (2015). "The relevance of EMT in breast cancer metastasis: Correlation or causality?" FEBS Lett **589**(14): 1577-1587.

Borden, K. L. (2008). "Pondering the puzzle of PML (promyelocytic leukemia) nuclear bodies: can we fit the pieces together using an RNA regulon?" Biochim Biophys Acta **1783**(11): 2145-2154.

Carracedo, A., D. Weiss, A. K. Leliaert, M. Bhasin, V. C. de Boer, G. Laurent, A. C. Adams, M. Sundvall, S. J. Song, K. Ito, L. S. Finley, A. Egia, T. Libermann, Z. Gerhart-Hines, P. Puigserver, M. C. Haigis, E. Maratos-Flier, A. L. Richardson, Z. T. Schafer and P. P. Pandolfi (2012). "A metabolic prosurvival role for PML in breast cancer." J Clin Invest **122**(9): 3088-3100.

Chen, T., Y. You, H. Jiang and Z. Z. Wang (2017). "Epithelial-mesenchymal transition (EMT): A biological process in the development, stem cell differentiation, and tumorigenesis." J Cell Physiol **232**(12): 3261-3272.

Cheng, X., Y. Liu, H. Chu and H. Y. Kao (2012). "Promyelocytic leukemia protein (PML) regulates endothelial cell network formation and migration in response to tumor necrosis factor alpha (TNFalpha) and interferon alpha (IFNalpha)." J Biol Chem **287**(28): 23356-23367.

de The, H. and Z. Chen (2010). "Acute promyelocytic leukaemia: novel insights into the mechanisms of cure." Nat Rev Cancer **10**(11): 775-783.

Diepenbruck, M. and G. Christofori (2016). "Epithelial-mesenchymal transition (EMT) and metastasis: yes, no, maybe?" Curr Opin Cell Biol **43**: 7-13.

Elisa de Stanchina, E. Q., Masako Narita, Ramana V. Davuluri,, G. F. Pier Paolo Pandolfi and a. S. W. Lowe (2004). "PML Is a Direct p53 Target that

Modulates p53 Effector Functions." Molecular Cell **13**.

Gonzalez, D. M. and D. Medici (2014). "Signaling mechanisms of the epithelial-mesenchymal transition." Sci Signal **7**(344): re8.

Hay, E. D. (1995). "An Overview of Epithelio-Mesenchymal Transformation." Acta Anat **154**.

Hoischen, C., S. Monajembashi, K. Weisshart and P. Hemmerich (2018). "Multimodal Light Microscopy Approaches to Reveal Structural and Functional Properties of Promyelocytic Leukemia Nuclear Bodies." Frontiers in Oncology **8**(125).

Hsu, K. S. and H. Y. Kao (2018). "PML: Regulation and multifaceted function beyond tumor suppression." Cell Biosci **8**: 5.

Hubackova, S., K. Krejcikova, J. Bartek and Z. Hodny (2012). "Interleukin 6 signaling regulates promyelocytic leukemia protein gene expression in human normal and cancer cells." J Biol Chem **287**(32): 26702-26714.

Kirsten Jensen, C. S. a. P. S. F. (2001). "PML protein isoforms and the RBCC/TRIM motif." Oncogene.

Lamouille, S., J. Xu and R. Derynck (2014). "Molecular mechanisms of epithelial-mesenchymal transition." Nat Rev Mol Cell Biol **15**(3): 178-196.

Martin-Martin, N., J. Sutherland and A. Carracedo (2013). "PML: Not all about Tumor Suppression." Frontiers in Oncology **3**(200).

Mazza, M. and P. G. Pelicci (2013). "Is PML a Tumor Suppressor?" Front Oncol **3**: 174.

Nisole, S., M. A. Maroui, X. H. Mascle, M. Aubry and M. K. Chelbi-Alix (2013). "Differential Roles of PML Isoforms." Front Oncol **3**: 125.
Prat, A. and C. M. Perou (2011). "Deconstructing the molecular portraits of breast cancer." Mol Oncol **5**(1): 5-23.
Prat, A., E. Pineda, B. Adamo, P. Galvan, A. Fernandez, L. Gaba, M. Diez, M. Viladot, A. Arance and M. Munoz (2015). "Clinical implications of the intrinsic molecular subtypes of breast cancer." Breast **24 Suppl 2**: S26-35.
Sachini, N., P. Arampatzi, A. Klonizakis, C. Nikolaou, T. Makatounakis, E. W. F. Lam, A. Kretsovali and J. Papamatheakis (2019). "Promyelocytic leukemia protein (PML) controls breast cancer cell proliferation by modulating Forkhead transcription factors." Molecular oncology **13**(6): 1369-1387.
Sahin, U., V. Lallemand-Breitenbach and H. de The (2014). "PML nuclear bodies: regulation, function and therapeutic perspectives." J Pathol **234**(3): 289-291.
Tetsu Kamitani, K. K., Hung Phi Nguyen, Hiroyoshi Wada, Taeko Fukuda-Kamitani, and and E. T. H. Yeh (1998). "Identification of Three Major Sentrinization Sites in PML." THE JOURNAL OF BIOLOGICAL CHEMISTRY **273**.
The, d. (1991). "The PML-RARa Fusion mRNA Generated by the t(l5;17) Translocation in Acute Promyelocytic Leukemia Encodes a Functionally Altered RAR." Cell **66**.

Chelbi-Alix, M. K., L. Pelicano, F. Quignon, M. H. Koken, L. Venturini, M. Stadler, J. Pavlovic, L. Degos and H. de The (1995). "Induction of the PML protein by interferons in normal and APL cells." Leukemia **9**(12): 2027-2033.

Fagioli, M., M. Alcalay, P. P. Pandolfi, L. Venturini, A. Mencarelli, A. Simeone, D. Acampora, F. Grignani and P. G. Pelicci (1992). "Alternative splicing of PML transcripts predicts coexpression of several carboxy-terminally different protein isoforms." Oncogene **7**(6): 1083-1091.